Analysis of two microearthquake swarms in Southeastern Sicily: evidence for active faults?

Luciano Scarfì ([1]), **Horst Langer** ([1]), **Giuseppe Di Grazia** ([1]), **Andrea Ursino** ([1]) and **Stefano Gresta** ([2])
([1]) *Istituto Nazionale di Geofisica e Vulcanologia, Sezione di Catania, Italy*
([2]) *Dipartimento di Scienze Geologiche, Università di Catania, Italy*

Abstract
Two microearthquake swarms occurring in Southeastern Sicily during November 1999 and January 2000 were analysed with respect to their seismotectonic features. Given the low magnitude of the events fault plane solutions for only four major events were computed, which revealed normal fault and inverse fault mechanisms. From the comparison of waveforms and the relation of *P*- and *S*-wave peak amplitudes, two families of multiplets were identified, each representing a distinct type of seismic dislocation. Composite fault plane solutions for the two families showed the same trends as for the single major events. The small number of mismatches of the composite solutions supports the hypothesis of two distinct types of seismic dislocation during the whole sequence, *i.e.* a normal fault mechanism along E-W striking planes and an inverse fault mechanism along NE-SW striking planes.

Key words *Southeastern Sicily – focal mechanisms – multiplet events – wave amplitude ratios – composite fault plane solutions*

1. Introduction

Since the early 1990's a new digital seismic network has been deployed in Southeastern Sicily in the framework of the «Poseidon Project» for monitoring the whole of Eastern Sicily (fig. 1). Southeastern Sicily was struck by large earthquakes in 1169 and 1693, each with a magnitude of about $M = 7$ (*e.g.*, Azzaro and Barbano, 2000), and most recently in 1990 by a moderate $M = 5.4$ earthquake (Amato *et al.*, 1995), which caused severe damage at a local scale. The earthquakes recorded by the network are of small magnitudes which have not yet exceeded $M = 4$. Despite the modest seismic energy release, the distribution of hypocenters may give useful seismotectonic hints as to the existence of active faults, orientation of seismic dislocations, relation of tectonic structures visible at the surface, depth distribution of hypocenters and so on.

In this study, we present the analyses carried out on two seismic swarms which occurred in November 1999 and January 2000 and we investigate the types of seismic dislocation. Given the small magnitudes of the events, fault plane solutions were obtained for only four events. They appear scarcely constrained as the number of first onset polarities available is limited. The significance of fault plane solutions can be proved compiling composite solutions where a number of events belonging to a swarm are culled together, provided that their hypocenters

Mailing address: Dr. Stefano Gresta, Dipartimento di Scienze Geologiche, Università di Catania, Corso Italia 55, 95129 Catania, Italy; e-mail: gresta@mbox.unict.it

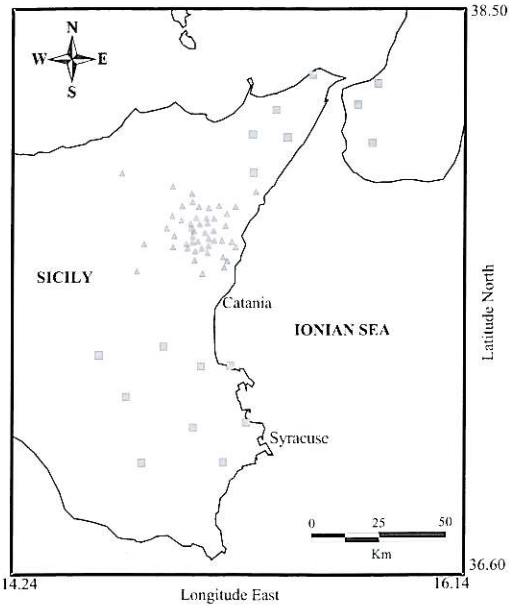

Fig. 1. Eastern Sicily seismic network. Triangles and squares mark the location of stations belonging to Etna, Messina Straits and Southeastern Sicily subnetworks, respectively.

are concentrated in the same area and they follow similar trends of seismic dislocation. Similarity measures will be obtained from the comparison of waveforms and the amplitude ratio of *P*- and *S*-waves. Indeed, it is a typical feature of the data set that many of the earthquakes can be addressed as multiplet events, forming groups with very similar waveforms. As the relation of *P*- and *S*-wave amplitudes depends strongly on the focal mechanisms, we will check whether the members of the families, identified on the base waveform correlation, can be assigned to one of the fault plane solutions calculated for the larger events of the two swarms. As a final step we will compile composite fault plane solutions for each family and compare them with the ones obtained for the single events. The number of polarities in agreement/disagreement in the composite solutions will be a further criterion for the significance of the claimed types of seismic dislocations during the swarm.

2. Structural features of the area

Eastern Sicily is characterised by a complex tectonic setting in the frame of the collisional process affecting the African-European convergent belt. The overall structure of this active zone is made up, from north to south, of three main structural units: the Sicilian compressional margin, the Gela-Catania foredeep and the Hyblean Plateau (Lentini, 1994, see fig. 2). The Hyblean area is part of the northern margin of the African plate which remained as a relatively undeformed foreland during the Neogene collisional process. It is bound to the east by the Malta escarpment, which forms one of the master faults in the Central Mediterranean, developing over 200 km from North Africa to Eastern Sicily. It represents a lithospheric fault system trending NNW-SSE, delimiting the continental crust of the African platform from the oceanic crust in the Ionian sea (Scandone *et al.*, 1981; Ben-Avram *et al.*, 1995; Hirn *et al.*, 1997). Northward, in the Gela-Catania foredeep, the margin of the Hyblean Plateau is downbended by a NE-SW fault system under the front of the Sicily mountain chain which is part of the Appennine-Maghrebian chain (Cogan *et al.*, 1989; Yellin-Dror *et al.*, 1997).

The data we are presenting concern earthquakes whose epicenters are found some kilometres to the north of the border between the Gela-Catania foredeep and the nappes of the Northern Chain. Significant local seismic activity in history is represented by the earthquakes of October 3, 1624 (M_s = 5-6) and December 23, 1959 (M_s = 4.5-5), with epicenters reported both at distances of *ca.* 10-15 km (see Azzaro and Barbano, 2000) from the earthquakes analysed here.

3. Analysis of data

The Southeastern Sicily Seismic Network (SESSN) consists of nine digital three-component stations, each equipped with short period Mark L4-3D seismometers having a natural frequency of 1.5 Hz and a damping of *ca.* 60% of critical. The data are sampled with a sampling frequency of 125 Hz; the corner frequency of the antialias filter is 51 Hz.

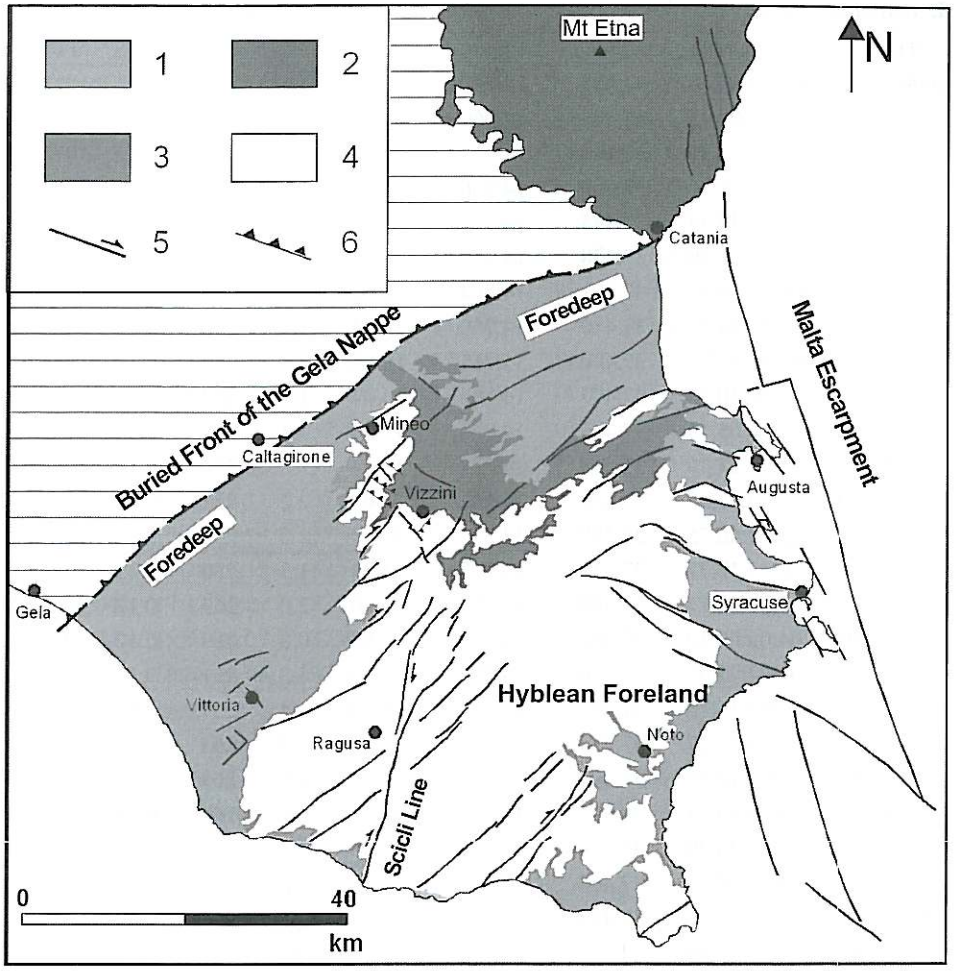

Fig. 2. Simplified geologic map of Southeastern Sicily (based on Carbone *et al.*, 1987; Grasso and Reuther, 1988; Lentini *et al.*, 1996). 1 = Recent-Quaternary deposits; 2 = late Pleistocene-Holocene Etnean volcanics; 3 = Plio-Pleistocene Hyblean volcanics; 4 = Meso-Cainozoic carbonate sediments; 5 = normal faults (strike-slip components shown by arrows); 6 = thrusts. Horizontal bars indicate the compressive domain of Appennine-Maghrebian chain (modified from Azzaro and Barbano, 2000).

Our data set consists of 57 events whose hypocenters are situated close to the most external chain folds, and whose focal depth range between 10 and 25 km (table I). A first swarm of 16 events was recorded on 19th and 20th November 1999. A second one (37 events) occurred on January 1 and 2, 2000. Isolated earthquakes followed on 3rd, 4th and 24th January.

3.1. *Location and magnitude*

The distribution of the epicenters follows grossly a N-S striking trend with a largest horizontal extension of about 7 km and a width of *ca.* 3 km (fig. 5). The epicenters of the first swarm are concentrated in the southern and central part of the area, while focal depths range

Table I. Earthquakes analysed in this study, their locations and relative parameters.

ID	Date	Origin time	Latitude	Longitude	Depth	M_L	Gap	RMS	ERZ	ERH
1	1999/11/19	02:46:50.40	37.465	14.749	19.56	1.5	260	0.07	3.7	2.3
2	1999/11/19	02:48:00.25	37.459	14.760	15.37	0.9	256	0.13	0.5	1.6
3	1999/11/19	04:33:14.75	37.466	14.763	14.56	2.2	259	0.2	0.4	1.0
4	1999/11/19	04:35:38.16	37.459	14.766	14.75	1.0	256	0.28	0.4	1.2
5	1999/11/19	05:22:43.34	37.445	14.765	14.55	2.2	251	0.22	0.5	1.3
6	1999/11/19	05:51:31.59	37.478	14.751	17.26	1.0	264	0.10	5.6	1.6
7	1999/11/19	06:09:28.03	37.471	14.764	14.61	1.6	260	0.14	0.4	1.1
8	1999/11/19	06:26:44.77	37.470	14.760	15.03	1.9	260	0.17	0.4	1.1
9	1999/11/19	06:33:17.78	37.470	14.761	15.06	1.5	260	0.17	0.4	1.1
10	1999/11/19	06:50:40.78	37.477	14.764	14.47	1.5	262	0.08	0.5	1.5
11	1999/11/19	07:44:05.19	37.445	14.768	15.36	1.4	251	0.08	0.5	1.8
12	1999/11/19	11:47:25.39	37.459	14.779	15.04	1.2	334	0.11	1.0	4.3
13	1999/11/19	13:00:37.52	37.451	14.762	14.68	2.2	253	0.19	0.4	0.9
14	1999/11/19	13:04:46.75	37.489	14.747	17.38	2.0	267	0.12	4.7	1.3
15	1999/11/19	16:38:13.37	37.443	14.768	14.84	1.3	250	0.23	0.7	1.9
16	1999/11/20	05:57:42.14	37.448	14.759	15.66	2.0	253	0.12	0.4	1.6
17	2000/01/01	04:02:00.10	37.496	14.750	15.52	0.8	269	0.12	0.6	1.8
18	2000/01/01	04:02:45.05	37.470	14.750	18.50	1.3	261	0.16	2.1	1.3
19	2000/01/01	04:03:18.76	37.457	14.750	20.70	1.4	257	0.08	1.6	2.3
20	2000/01/01	04:04:27.27	37.474	14.751	17.68	1.4	263	0.14	2.4	1.3
21	2000/01/01	04:07:12.85	37.498	14.754	15.28	0.9	269	0.13	0.8	2.0
22	2000/01/01	04:08:54.14	37.471	14.752	17.76	1.1	262	0.16	2.3	1.4
23	2000/01/01	04:11:24.20	37.474	14.750	17.58	1.5	262	0.15	2.3	1.3
24	2000/01/01	04:15:02.32	37.464	14.754	15.82	1.2	259	0.18	0.4	1.4
25	2000/01/01	04:15:51.65	37.449	14.755	20.22	1.5	254	0.10	1.4	2.1
26	2000/01/01	04:19:16.60	37.497	14.753	15.40	0.9	269	0.10	0.6	1.8
27	2000/01/01	04:22:39.45	37.467	14.753	15.80	2.0	260	0.17	0.4	1.3
28	2000/01/01	04:25:07.27	37.472	14.751	18.56	1.4	262	0.16	2.1	1.4
29	2000/01/01	05:06:33.29	37.472	14.750	18.61	1.6	262	0.17	2.1	1.4
30	2000/01/01	05:41:00.75	37.452	14.750	23.26	0.8	255	0.05	2.1	2.9
31	2000/01/01	05:41:18.43	37.470	14.751	18.49	1.3	261	0.16	2.1	1.3
32	2000/01/01	05:42:23.84	37.463	14.755	15.73	1.2	258	0.19	0.4	1.5
33	2000/01/01	05:58:58.32	37.482	14.755	15.40	0.9	264	0.13	0.5	1.5
34	2000/01/01	06:22:06.04	37.498	14.755	15.42	0.9	269	0.12	0.7	1.8
35	2000/01/01	07:11:03.23	37.495	14.755	15.28	0.8	268	0.12	0.8	1.9
36	2000/01/01	07:13:01.69	37.454	14.753	20.64	1.9	269	0.11	1.8	2.3
37	2000/01/01	08:15:18.27	37.469	14.750	17.60	0.8	261	0.18	2.5	1.5
38	2000/01/01	09:57:08.03	37.488	14.760	15.13	0.7	276	0.18	0.8	1.9
39	2000/01/01	10:02:19.09	37.458	14.749	22.93	1.0	258	0.08	2.0	2.9

Table I (*continued*).

ID	Date	Origin time	Latitude	Longitude	Depth	M_L	Gap	RMS	ERZ	ERH
40	2000/01/01	10:03:02.64	37.495	14.750	15.72	1.6	269	0.12	0.6	2.0
41	2000/01/01	10:27:53.92	37.482	14.753	15.83	1.1	265	0.13	0.4	1.4
42	2000/01/01	10:33:45.55	37.495	14.756	15.48	0.8	268	0.11	0.6	1.8
43	2000/01/01	10:35:54.04	37.496	14.756	15.34	0.8	268	0.12	0.6	1.8
44	2000/01/01	23:00:14.95	37.491	14.763	14.34	1.2	266	0.14	0.7	1.6
45	2000/01/01	23:02:10.18	37.486	14.759	15.07	1.5	265	0.13	0.6	1.6
46	2000/01/02	07:20:28.32	37.498	14.754	15.22	0.8	269	0.11	0.6	1.8
47	2000/01/02	07:36:30.25	37.475	14.750	18.53	1.4	263	0.15	2.1	1.4
48	2000/01/02	07:53:43.72	37.473	14.748	18.75	1.7	263	0.16	1.9	1.3
49	2000/01/02	08:04:53.57	37.470	14.751	18.00	1.5	261	0.16	2.0	1.4
50	2000/01/02	08:38:09.03	37.459	14.744	16.32	1.3	293	0.07	2.8	1.4
51	2000/01/02	09:24:40.03	37.463	14.741	22.90	2.0	260	0.14	2.1	1.3
52	2000/01/02	10:28:38.11	37.479	14.757	15.77	1.2	263	0.07	0.9	2.6
53	2000/01/02	12:07:46.94	37.467	14.745	21.16	1.6	261	0.12	2.2	1.2
54	2000/01/03	04:28:18.15	37.505	14.747	18.01	0.7	282	0.08	0.7	2.3
55	2000/01/04	19:42:55.21	37.500	14.747	15.81	1.3	270	0.08	0.6	2.3
56	2000/01/24	15:51:46.57	37.451	14.762	15.49	1.0	254	0.15	0.5	2.0
57	2000/01/24	16:38:08.03	37.469	14.765	14.37	2.5	259	0.15	0.4	1.2

from 14 to 16 km. The epicenters of the second swarm follow a N-S striking direction and appear slightly shifted to the west with respect to those of the former swarm. The focal depths scatter in a range between 14 and 24 km. On the other hand the hypocenters of the two events on 24th January belong to the cluster of the first swarm (figs. 3 and 4a,b).

Although the magnitudes of these events are quite small, *i.e.* between 0.8 and 2.5, the signal to noise ratio, in terms of displacement, is at least 40 dB on all three components. The locations were obtained by the HYPOELLIPSE program (Lahr, 1989) using the velocity model by Sharp *et al.* (1980). Their accuracy is about 1.5 km both for the epicentral coordinates and the focal depth. Figure 5 shows the locations of the earthquake epicenters and seismic stations on the Hyblean Plateau. Five out of the nine stations are close to the epicenters, which explains the fair accuracy of the hypocenter locations despite of the somewhat unfavourable geometry.

The local magnitude was computed using the formula (see Lahr, 1989)

$$M_L = \log(A/2) - 0.15 + 0.80 \cdot \log^2 X$$

where A is the maximum peak to peak amplitude in millimetres as recorded on a standard Wood-Anderson seismograph and X is the hypocentral distance in kilometres.

Radiated seismic energy was obtained using the empirical formula: $\log E = 9.9 + 1.9M - 0.024M^2$ (Richter, 1958), where E is the energy expressed in Joules and M is the local magnitude. Figure 6 shows the seismic energy progressively radiated from each event, expressed in percentage of the total energy released during the two swarms. About 88% of the total energy was released by 11 earthquakes. These correspond to earthquakes with magnitude above 1.6, of which six occurred during the swarm of November 1999 and four on the first days of January 2000. After a period of quiescence of almost three weeks, the sequence finished with two events on 24th January, the latter having a magnitude of 2.5.

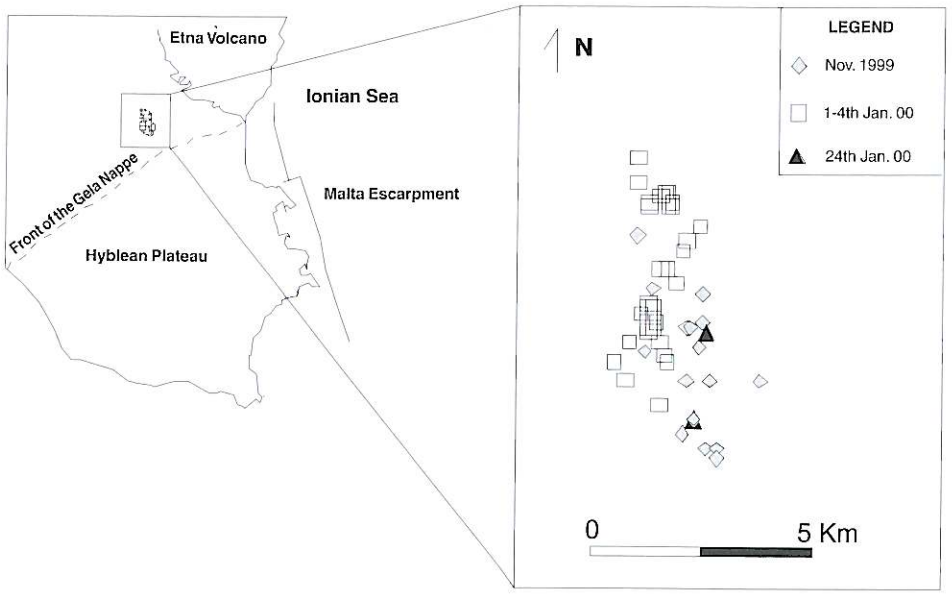

Fig. 3. Epicentral map of the used data set.

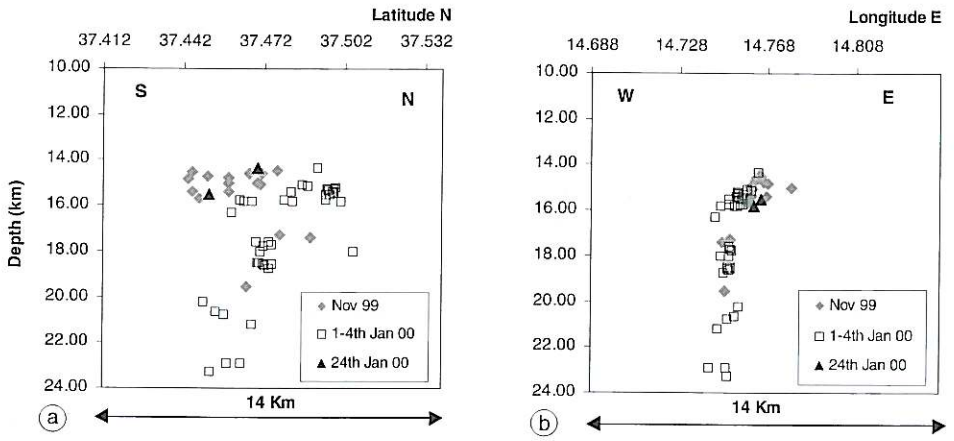

Fig. 4a,b. Hypocentral distribution of the whole seismic sequence. a) N-S section; b) E-W section. Different symbols correspond to various time periods of occurrence (see legend).

3.2. *Fault plane solutions*

Fault plane solutions were computed for four major events of the swarms using the FPFIT program (Reasenberg and Oppenheimer, 1985). For this purpose we added the *P*-onset readings from seismic stations deployed on the neighbouring Mt. Etna volcano, collecting up to 12 *P*-onsets. The velocity model used for the computation of the azimuths and incident angles is the same model as used for the location.

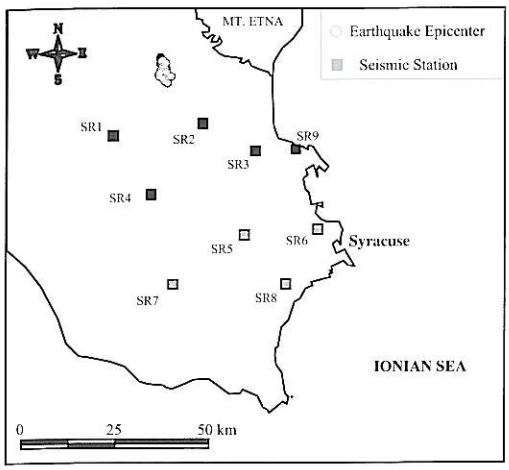

Fig. 5. Geographical distribution of the earthquake epicenters and seismic stations that recorded the events. Black squares indicate the stations with the major number of phases used for the hypocenter locations.

The results of the fault plane solutions are given in table II and fig. 7. Both events on 19th November and 24th January reveal normal faulting mechanisms along E-W striking planes, with an almost vertical *P*-axis. On the other hand, the earthquakes on 1st and 2nd January show a thrust mechanism along NE-SW striking planes, with an almost NW striking *P*-axis. As stated earlier, the hypocenters of the earthquakes on 24th January belong to the cluster of the first swarm on 19th and 20th November, whereas the events of 1st and 2nd January should be assigned to the second cluster. Given the limited number of polarities and the western network gap, one can certainly argue the reliability of the fault plane solutions. Nevertheless, it is noteworthy that the fault plane solutions carried out for the representative events of the corresponding clusters converge fairly well. The number of polarities available for the event on 19th November is higher than for those of the second swarm, where the polarities at two stations

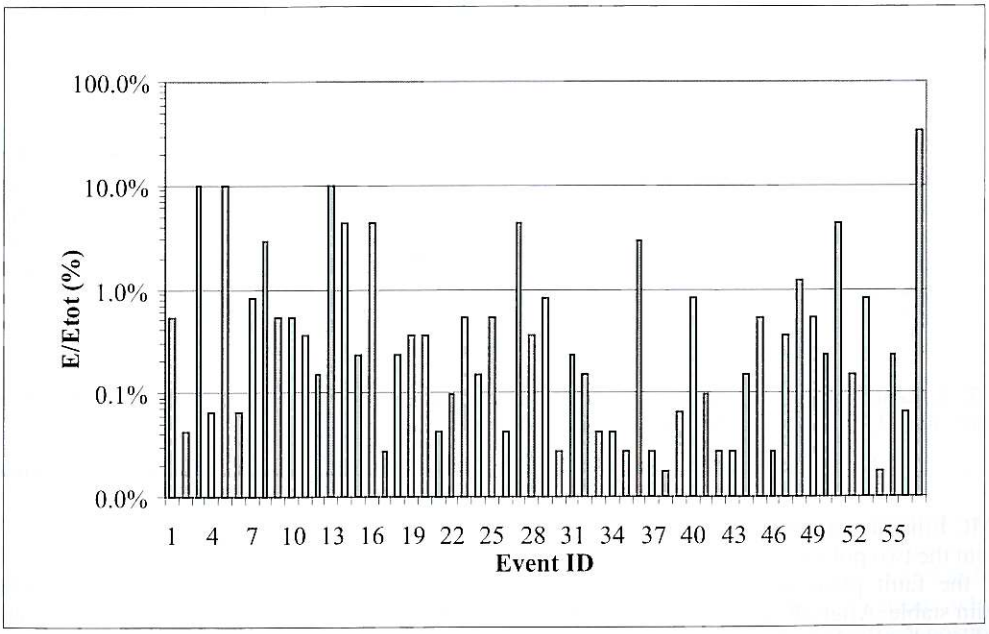

Fig. 6. Relative radiated seismic energy by the single event. 100% corresponds to the total energy released during the two swarms.

Table II. Fault plane solutions carried out for four major events of the two swarms.

ID	Date	Origin time	1st Plane		
			Dip direction	Dip	Rake
5	1999/11/19	05:22:43.34	165	45	110
57	2000/01/24	16:38:08.03	190	65	110
36	2000/01/01	07:13:01.69	165	40	140
51	2000/01/02	09:24:40.03	150	25	120

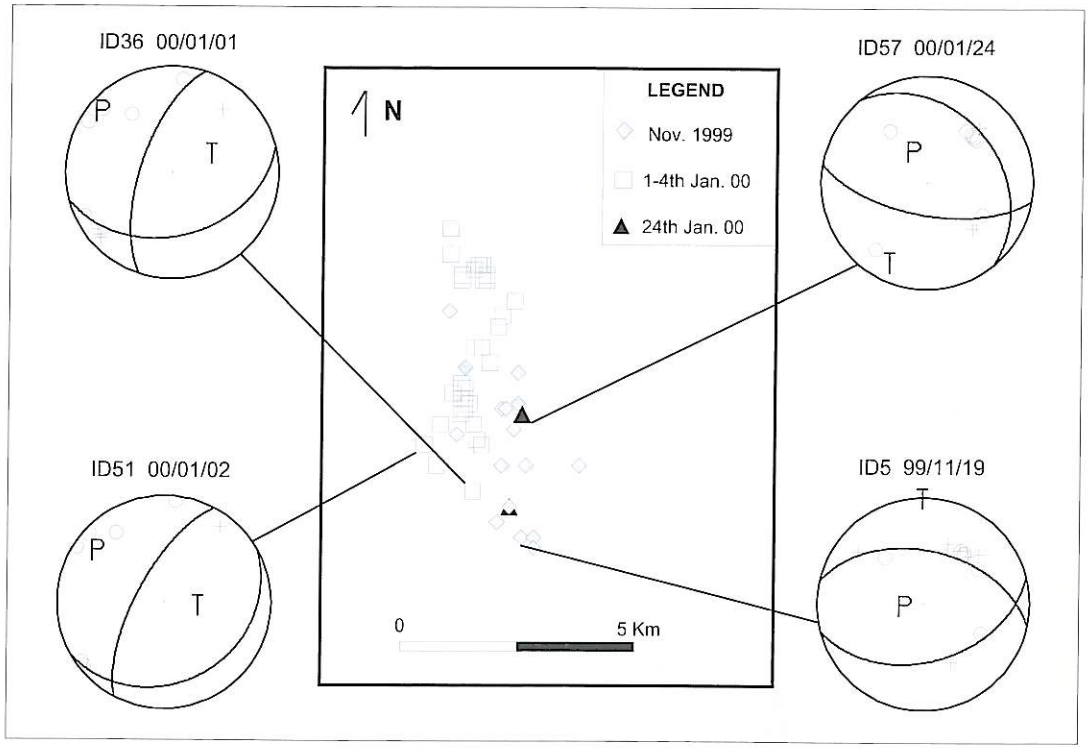

Fig. 7. Epicentral map and focal mechanism (lower hemisphere projection) of the events of table II (+ for compression; O for dilatation). See the text for further explanations.

on Mt. Etna are missing. In an experiment we left out the two polarities of Mt. Etna. Nevertheless, the fault plane solutions for event n. 5 remain stable. After all, we may state as a working hypothesis that the two clusters indeed reflect two distinct mechanisms of seismic dislocation.

3.3. *Waveforms and amplitude ratios*

In order to verify our working hypothesis that the two clusters may indeed represent two different types of seismic dislocation we compared waveforms and amplitude ratios of *P*- and *S*-waves of the clusters.

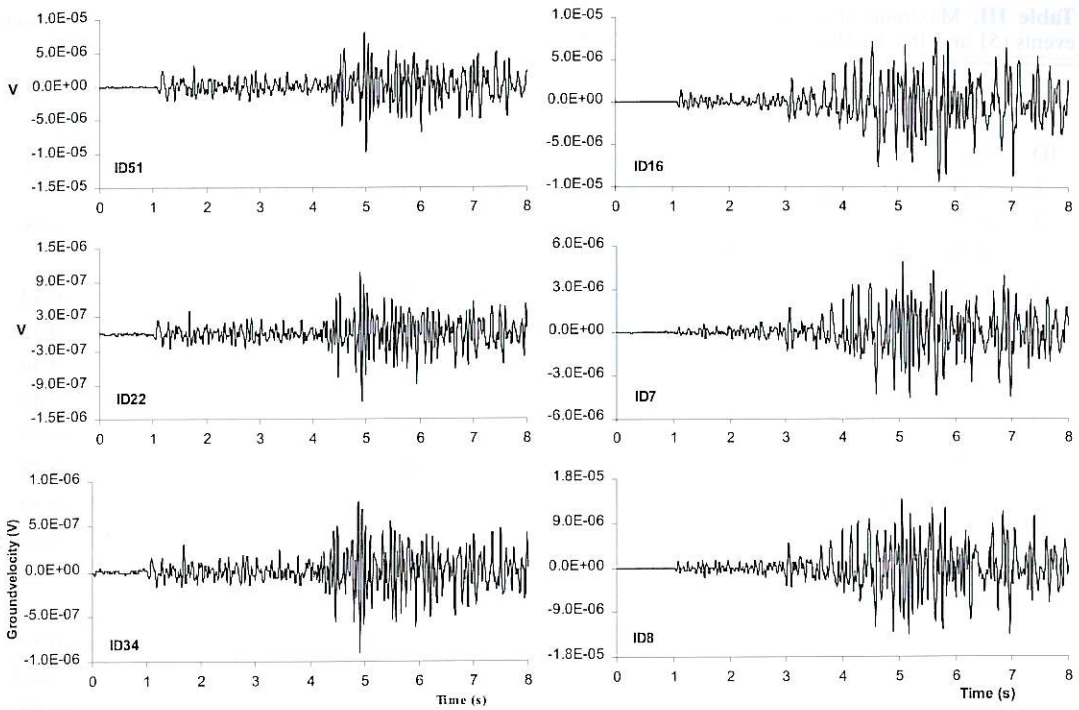

Fig. 8. A comparison between events recorded at SR2 station (vertical component). On the right, three earthquakes of the first cluster; on the left, events of the second cluster. Note the high waveform similarity between events of the same cluster.

A crude visual inspection reveals surprising similarities of waveforms for the events belonging to the same cluster (fig. 8), despite significant magnitude differences and the scatter of hypocentral coordinates. As a simple measure, we used the maximum of the cross-correlation function between the seismic traces which were calculated using PITSA 3.0 by Scherbaum and Johnson (1992). For each of the two clusters, we defined a master event, *i.e.* the event with the best signal to noise ratio. We then calculated the cross-correlation functions of the other events with respect to the two master events. We considered the vertical component seismograms of three key stations, *i.e.* SR1, SR2, and SR3. These key stations recorded almost all of the 57 events of our data set. We identified the events n. 16 and n. 51 in table I as master events for the two corresponding clusters and calculated the cross-correlation functions for 8 s windows starting 1.0 s before the *P*-wave onset. The maximum values of the cross-correlation functions reported in table III show that all events occurring in November are highly similar to the master event n. 16, whereas the cross-correlation with the master event n. 51 is quite low. On the other hand, most of the events belonging to the latter swarm show high correlation coefficients with the master event n. 51. However, the events on 24th January (n. 57 and 58 of table III) are similar to the master event n. 16. This confirms that they cluster with the first swarm from both hypocentral coordinates and focal mechanism.

Slight differences in the cross-correlation values can be noted for the various stations, which is partly due to the different geometrical position of the stations with respect to the hypocenters. Both SR2 and SR3 are SE located with respect to the epi-

Table III. Maximum absolute values of the cross-correlation functions of the events with respect to the master events (51 and 16), for three stations (SR1, SR2, SR3).

	Cluster of November							Cluster of January						
	SR1		SR2		SR3			SR1		SR2		SR3		
ID	51	16	51	16	51	16	ID	51	16	51	16	51	16
1	0.20	0.77	0.22	0.69	0.32	0.76	17	0.94	0.19	0.81	0.17	–	–
2	0.22	0.77	0.23	0.68	0.28	0.71	20	0.97	0.20	0.92	0.24	0.90	0.46
3	0.25	0.87	0.20	0.80	0.41	0.89	21	0.96	0.19	0.86	0.23	–	–
4	0.20	0.90	0.23	0.82	0.43	0.90	22	0.98	0.21	0.96	0.24	0.89	0.42
5	0.23	0.64	0.27	0.59	0.44	0.64	23	0.96	0.20	0.79	0.19	0.85	0.42
6	0.18	0.72	0.22	0.67	0.35	0.81	24	0.96	0.21	0.62	0.21	0.79	0.49
7	0.20	0.94	0.24	0.89	0.43	0.92	26	0.95	0.21	0.87	0.24	0.81	0.38
8	0.20	0.95	0.26	0.94	0.44	0.94	27	0.95	0.21	0.78	0.19	0.82	0.43
9	0.24	0.95	0.24	0.91	0.45	0.91	29	0.86	0.22	0.81	0.23	0.86	0.45
13	0.22	0.91	0.29	0.83	0.46	0.91	32	0.93	0.20	0.69	0.18	0.75	0.40
15	0.20	0.85	0.27	0.86	0.41	0.89	33	0.92	0.19	0.68	0.17	0.71	0.38
16	0.21	–	0.26	–	0.47	–	34	0.97	0.21	0.92	0.25	0.90	0.40
56	0.26	0.60	0.21	0.52	0.34	0.70	35	0.94	0.18	0.80	0.18	–	–
57	0.28	0.78	0.22	0.67	0.44	0.86	36	0.81	0.27	0.67	0.19	0.68	0.33
							37	0.89	0.20	0.62	0.16	–	–
							38	0.92	0.21	0.69	0.17	0.52	0.30
							41	0.93	0.20	0.72	0.20	0.77	0.48
							42	0.94	0.18	0.79	0.19	0.79	0.40
							43	0.94	0.19	0.76	0.19	0.64	0.36
							44	0.90	0.22	0.58	0.17	0.75	0.48
							46	0.94	0.19	0.83	0.19	0.78	0.39
							47	0.98	0.20	0.91	0.23	0.94	0.48
							48	0.97	0.21	0.85	0.22	0.88	0.49
							49	0.98	0.20	0.87	0.22	–	–
							53	0.93	0.21	0.70	0.23	0.75	0.54
							54	0.93	0.21	0.74	0.19	0.59	0.32
							55	0.90	0.22	0.65	0.18	0.75	0.45

centers, whereas SR1 lies in a SW direction. Results are probably also influenced by site effects. The displacement spectra of the signals recorded at station SR1 exhibit a bandlimitation between 2 and 5 Hz, whereas the spectra of the same signals recorded at SR2 are flat between 2 and 20 Hz. The lower limit can be due to the instrumental response, whereas the high-frequency cut-off of 5 Hz at SR1 is supposed to reflect a site effect.

Finally, we calculated the matrix of maximum cross-correlation coefficients for all events reported in table III. For the sake of clarity we reorganised the data set in a way that events of 24th January, 2000 cluster with the ones of November 1999. The matrix of cross-correlation coefficients is graphically visualised in fig. 9 for station SR1. Similar outlines were obtained for matrices of station SR2 and SR3. The

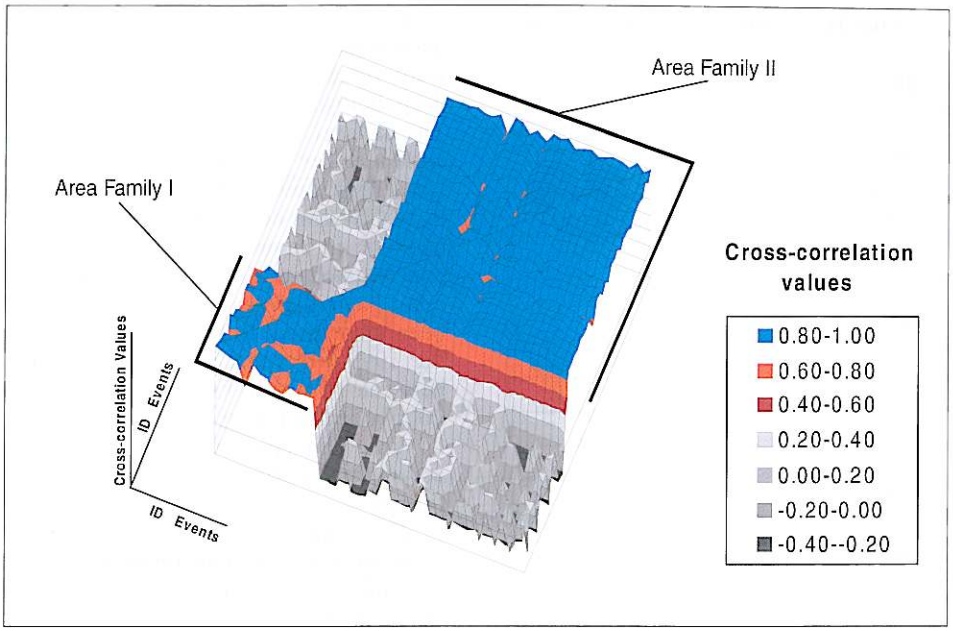

Fig. 9. Graphical visualisation of the correlation matrix obtained for station SR1. The tabled values of the matrix are given in the Appendix.

graph confirms the hypothesis of two distinct groups since high correlation coefficients are observed only among records which belong to the same families.

Waveforms and in particular the peak amplitudes of *P*- and *S*-waves depend strongly on the focal mechanism. Here we considered the peak amplitudes of *P*-waves measured on the vertical component and the maximum horizontal *S*-wave amplitudes. The latter ones were obtained forming the average of the peak amplitudes on the two horizontal components. We considered again the key stations SR1, SR2 and SR3. At SR1 the *P*/*S*-wave ratios for events of the swarm in November 1999 tend to be higher than those of the latter swarm. Some events of the former swarm, however, show similar values as the events of the second group, and *vice versa*. At the stations SR2 and SR3, the *P*/*S* amplitude wave ratios of the former swarm are clearly lower than those of the latter swarm. As before we note that the events of 24th January show the same features as the cluster of November 1999 (fig. 10).

3.4. *Composite fault plane solutions*

Two composite fault plane solutions were obtained by combining the *P*-onset polarities of the two families defined on the basis of waveform analysis and *P*/*S*-wave amplitude ratios (fig. 11) and table IV. The composite solutions fit well the solutions found for the single major master events of the two swarms. The composite solution for the first family shows 9 polarities out of a total of 63 in disagreement, the solution for the second family only 6 polarities out of 90 in disagreement. The small number of not fitting polarities in the composite solutions is an additional support for the existence of two distinct seismic dislocations well linked to the two swarms.

4. Discussion and conclusions

Eastern Sicily is a region characterised by a strong regional stress due to the convergent

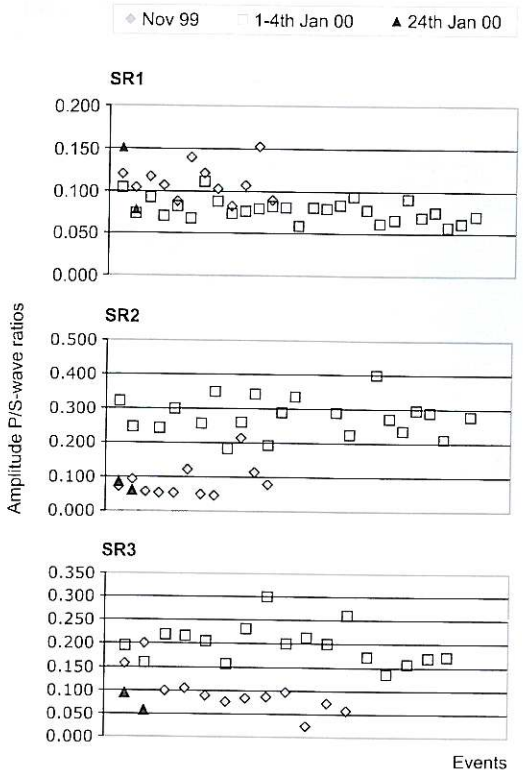

Fig. 10. Plot of amplitude *P*/*S*-wave ratios at three key stations (SR1, SR2, SR3). Diamonds, squares and triangles indicate the different periods of earthquake occurrence. Note different trends for the events of November and January.

motion of the European and African plates (Richardson *et al.*, 1979; Müller *et al.*, 1992; Ward, 1994). It is one of the most seismically active zones of Italy. It was struck several times by violent seismic events (Azzaro and Barbano, 2000; Boschi *et al.*, 1995, 1997), spaced out by long periods of quiescence, at least apparently because there are no data of a local seismic network until 1994.

Indeed, the destructive earthquakes have not yet been related to well defined active faults (Bianca *et al.*, 1999; Sirovich and Pettenati, 1999), and only after the last moderate 1990 earthquake have the first instrumental recordings for this seismogenic area been available.

In this work we investigated a seismic sequence which occurred some kilometres northward from the border the Gela-Catania foredeep, below the thrust zone (Ragg *et al.*, 1999). The data set is composed of microearthquakes with a rather irregular distribution of energy. Local magnitudes did not exceed 2.5. Essentially, two swarms occurred: one in November 1999 and one in January 2000. Hypocenters were concentrated in a relatively small crustal volume. Nevertheless, two distinct clusters have been recognised. In fact, the events of November 1999 were concentrated in a depth range between 14 and 16 km, while those of January 2000 occurred also at greater depth, up to 25 km. The epicenters of the latter swarm are slightly shifted to NW with respect to the former.

The comparison of the waveforms recorded at the three key stations revealed a high degree of similarity between earthquakes belonging to the same swarm. The cross-correlation coefficients showed clearly that the two swarms form two distinct families made up by multiplets. The two earthquakes which resumed on 24th January, belong to the family of the first swarm, with respect to both locations and waveforms. The existence of two families was also confirmed by the focal mechanisms of four major events. The solutions for the earthquakes occurred on 19th November 1999 and on 24th January 2000 showed a mechanism corresponding to a normal fault, whose fault planes strike in an E-W direction, with a vertical *P*-axis. For the two other events on 1st and 2nd January 2000 fault planes solutions revealed an inverse fault along NE-SW striking planes, with an almost horizontal *P*-axis, striking NW-SE. Moving on from the

Table IV. Composite fault plane solutions carried out for the two earthquakes families.

	1st Plane		
	Dip direction	Dip	Rake
Composite solution 1st family	170	50	100
Composite solution 2nd family	145	45	100

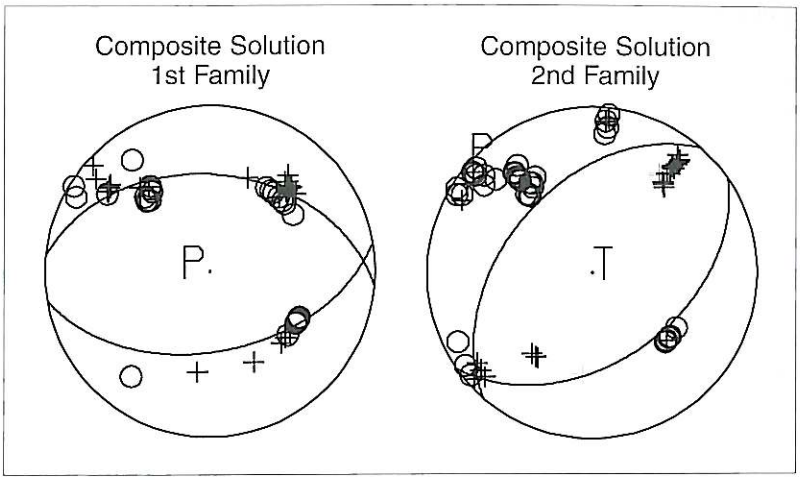

Fig. 11. Composite fault plane solution of the two earthquakes families.

similarities of the waveforms of events belonging to the same group we conclude that the two families indeed represent two different types of fault mechanism. This conclusion is confirmed by the comparison of the *P*/*S*-wave amplitude ratios and composite fault plane solutions. Similar to the results obtained by the comparison of the waveforms, we notice separate trends for the two earthquake families, where the two events of 24th January belong to the family of the first swarm. Also the composite fault plane solutions computed for the two earthquake families fit well to the solutions found for the four major events of the data set. The small number of mismatching polarities is an additional support for claiming the existence of two distinct types of seismic dislocation for our data set. The two mechanisms are given (i) as a normal fault and (ii) an inverse fault.

Some information on the orientation of *in situ* tectonic stress in the area can be deduced from borehole breakout analysis by Ragg *et al.* (1999). They detected a nearly NNW orientation for the maximum horizontal stress (SH_{max}) on the Hyblean Plateau, while a NE direction was found on the Gela nappe (see details in Ragg *et al.*, 1999, table 1). The authors explained the locally differing observed stress orientations as due to the modulation by crustal thickness variations and local sources of a regional, NW oriented, stress field.

Breakout data available for a site (the «Ramacca well») located only about one kilometre from the area affected by the seismic sequence have been studied. Data were collected in a log interval depth range from 247 to 1267 m, so they refer to the very shallow part of the crust; the identified stress orientation (SH_{max}) was N66E (Ragg *et al.*, 1999).

Conversely, the two well identified seismic clusters showed the coexistence of two differing faulting mechanisms in the same small (about 200 km^3) volume of deeper crust. Moreover, the *P*-axes obtained from both single and composite fault plane solutions, resulted almost vertically oriented for the former cluster and almost horizontal, NW striking for the latter. These results disagree with the above quoted local and shallow stress field, while they are in agreement with the proposed regional one (Ragg *et al.*, 1999).

Acknowledgements

We are indebted with Dr. Rita Di Giovambattista (Istituto Nazionale di Geofisica e Vulcanologia, Rome) for her useful comments on the paper.

Appendix. Matrix of cross-correlation coefficients.

ID	1	2	3	4	5	6	7	8	9	13	15	16	56	57	17	20	21	22	23	24	26
1	1.00	0.96	0.91	0.89	0.61	0.94	0.83	0.82	0.72	0.71	0.83	0.78	0.79	0.79	-0.20	-0.20	-0.21	0.21	-0.20	-0.21	-0.20
2	0.96	1.00	0.90	0.88	0.61	0.90	0.83	0.81	0.74	0.70	0.84	0.78	0.81	0.79	-0.22	-0.22	-0.23	-0.22	-0.22	-0.24	-0.22
3	0.91	0.90	1.00	0.93	0.71	0.90	0.89	0.85	0.84	0.79	0.86	0.87	0.79	0.88	-0.25	-0.24	-0.24	0.25	0.24	-0.25	-0.24
4	0.89	0.88	0.93	1.00	0.63	0.87	0.96	0.91	0.89	0.81	0.85	0.90	0.71	0.83	-0.22	-0.21	-0.21	-0.21	-0.22	-0.24	0.21
5	0.61	0.61	0.71	0.63	1.00	0.60	0.59	0.56	0.65	0.65	0.65	0.64	0.53	0.67	-0.24	-0.24	-0.23	-0.24	-0.24	-0.25	-0.24
6	0.94	0.90	0.90	0.87	0.60	1.00	0.79	0.75	0.68	0.68	0.82	0.73	0.79	0.78	-0.21	-0.20	-0.18	-0.20	-0.18	-0.19	-0.20
7	0.83	0.83	0.89	0.96	0.59	0.79	1.00	0.97	0.92	0.84	0.85	0.94	0.64	0.79	-0.21	-0.20	-0.20	-0.20	-0.21	-0.22	0.19
8	0.82	0.81	0.85	0.91	0.56	0.75	0.97	1.00	0.93	0.87	0.85	0.96	0.61	0.75	-0.21	-0.20	-0.20	0.21	-0.21	-0.22	0.20
9	0.72	0.74	0.84	0.89	0.65	0.68	0.92	0.93	1.00	0.89	0.82	0.96	0.56	0.74	-0.23	-0.22	-0.23	-0.22	-0.23	-0.23	0.21
13	0.71	0.70	0.79	0.81	0.65	0.68	0.84	0.87	0.89	1.00	0.85	0.92	0.54	0.69	0.22	0.22	0.22	0.23	0.22	0.23	0.20
15	0.83	0.84	0.86	0.85	0.65	0.82	0.85	0.85	0.82	0.85	1.00	0.86	0.69	0.71	0.20	0.21	0.20	0.21	-0.21	0.20	0.18
16	0.78	0.78	0.87	0.90	0.64	0.73	0.94	0.96	0.96	0.92	0.86	1.00	0.61	0.78	-0.20	-0.21	-0.20	0.21	0.21	-0.21	0.21
56	0.79	0.81	0.79	0.71	0.53	0.79	0.64	0.61	0.56	0.54	0.69	0.61	1.00	0.86	-0.28	-0.28	-0.26	-0.28	-0.24	-0.24	-0.29
57	0.79	0.79	0.88	0.83	0.67	0.78	0.79	0.75	0.74	0.69	0.71	0.78	0.86	1.00	-0.30	-0.30	-0.27	-0.29	-0.27	-0.27	-0.30
17	-0.20	-0.22	-0.25	-0.22	-0.24	-0.21	-0.21	-0.21	-0.23	0.22	0.20	-0.20	-0.28	-0.30	1.00	0.97	0.94	0.94	0.96	0.95	0.94
20	-0.20	-0.22	-0.24	-0.21	-0.24	-0.20	-0.20	-0.20	-0.22	0.22	0.21	-0.21	-0.28	-0.30	0.97	1.00	0.97	0.96	0.98	0.95	0.96
21	-0.21	-0.23	-0.24	-0.21	-0.23	-0.18	-0.20	-0.20	-0.23	0.22	0.20	-0.20	-0.26	-0.27	0.94	0.97	1.00	0.97	0.96	0.94	0.97
22	0.21	-0.22	0.25	-0.21	-0.24	-0.20	-0.20	0.21	-0.22	0.23	0.21	0.21	-0.28	-0.29	0.94	0.96	0.97	1.00	0.95	0.94	0.98
23	-0.20	-0.22	0.24	-0.22	-0.24	-0.18	-0.21	-0.21	-0.23	0.22	-0.21	0.21	-0.24	-0.27	0.96	0.98	0.96	0.95	1.00	0.96	0.93
24	-0.21	-0.24	-0.25	-0.24	-0.25	-0.19	-0.22	-0.22	-0.23	0.23	0.20	-0.21	-0.24	-0.27	0.95	0.95	0.94	0.94	0.96	1.00	0.92
26	-0.20	-0.22	-0.24	0.21	-0.24	-0.20	0.19	0.20	0.21	0.20	0.18	0.21	-0.29	-0.30	0.94	0.96	0.97	0.98	0.93	0.92	1.00
27	0.20	-0.22	-0.24	-0.23	-0.25	-0.19	-0.22	-0.22	-0.25	0.23	-0.21	-0.23	-0.23	-0.27	0.97	0.96	0.92	0.93	0.98	0.98	0.91
29	0.26	0.26	0.28	-0.24	-0.26	0.22	-0.22	0.21	0.22	0.23	0.24	0.22	0.24	0.27	0.82	0.84	0.84	0.86	0.81	0.84	0.85
32	0.20	-0.22	-0.23	0.22	-0.23	0.20	0.20	0.20	-0.23	0.21	0.20	-0.21	0.25	-0.26	0.94	0.95	0.95	0.93	0.97	0.92	0.92
33	0.20	-0.22	0.24	-0.22	0.24	0.22	-0.22	-0.21	-0.25	0.23	-0.20	-0.23	0.24	0.26	0.94	0.93	0.92	0.91	0.96	0.93	0.89
34	0.21	-0.23	0.25	-0.21	-0.23	-0.19	-0.20	0.22	-0.21	0.22	0.21	0.21	-0.29	-0.30	0.91	0.96	0.96	0.98	0.92	0.92	0.97
35	-0.19	-0.21	-0.23	-0.21	-0.24	-0.19	-0.20	-0.19	-0.21	-0.20	-0.20	-0.20	-0.26	-0.29	0.96	0.98	0.96	0.95	0.96	0.93	0.95
36	0.25	0.25	0.26	0.28	-0.26	0.22	0.29	0.27	0.29	0.23	-0.23	0.28	0.29	0.31	0.83	0.84	0.81	0.81	0.85	0.80	0.79
37	0.21	-0.22	0.24	-0.21	0.24	0.22	-0.20	-0.20	-0.25	0.22	0.21	-0.23	0.23	0.26	0.91	0.92	0.90	0.89	0.93	0.89	0.86
38	0.21	-0.21	0.22	0.23	-0.25	0.19	0.21	0.21	-0.24	0.21	0.20	0.21	0.23	0.24	0.91	0.95	0.94	0.91	0.95	0.92	0.90
41	0.20	-0.22	-0.22	0.22	0.23	0.21	-0.20	0.20	-0.23	0.21	0.20	0.21	-0.24	-0.26	0.92	0.96	0.95	0.93	0.96	0.92	0.91
42	-0.20	-0.20	-0.24	-0.21	-0.23	-0.19	-0.19	0.18	-0.21	-0.19	0.18	-0.19	-0.28	-0.30	0.94	0.97	0.96	0.94	0.93	0.92	0.96
43	0.20	-0.22	-0.23	0.21	-0.22	0.17	-0.19	0.19	0.21	0.19	0.20	0.19	0.23	-0.25	0.92	0.96	0.96	0.94	0.94	0.92	0.94
44	0.21	-0.23	0.26	-0.24	-0.28	0.24	-0.23	-0.23	-0.28	-0.25	0.22	-0.26	-0.25	0.27	0.88	0.89	0.87	0.87	0.93	0.93	0.84
46	0.19	-0.20	-0.22	0.21	-0.23	-0.18	0.18	0.19	-0.20	-0.19	-0.19	0.19	-0.27	-0.29	0.91	0.95	0.96	0.95	0.92	0.90	0.96
47	-0.19	-0.22	0.24	-0.21	-0.24	-0.18	-0.20	-0.20	-0.25	0.22	-0.21	-0.22	-0.25	-0.27	0.92	0.95	0.95	0.97	0.95	0.96	0.95
48	0.20	-0.22	0.24	-0.22	-0.24	0.19	-0.21	-0.20	-0.25	0.22	-0.21	-0.23	-0.23	-0.26	0.95	0.97	0.95	0.95	0.97	0.97	0.93
49	-0.20	-0.20	-0.24	-0.20	-0.25	-0.19	-0.19	0.20	-0.23	-0.22	-0.22	-0.21	-0.26	-0.28	0.94	0.97	0.95	0.97	0.97	0.96	0.94
51	0.21	-0.23	0.25	-0.22	-0.24	-0.19	-0.21	-0.21	-0.24	0.23	0.21	0.22	-0.27	-0.28	0.94	0.97	0.97	0.99	0.96	0.97	0.96
53	-0.21	-0.23	-0.25	-0.24	-0.25	0.20	-0.23	-0.22	-0.25	-0.22	-0.21	-0.23	-0.24	-0.26	0.91	0.93	0.93	0.93	0.94	0.91	0.91
54	0.18	0.20	-0.21	0.21	-0.23	-0.17	-0.20	0.22	-0.24	0.21	-0.19	-0.22	-0.23	-0.25	0.88	0.91	0.94	0.94	0.89	0.89	0.94
55	0.21	-0.22	0.23	0.23	-0.25	0.22	0.22	0.21	-0.25	0.22	0.21	-0.23	-0.24	0.26	0.90	0.91	0.91	0.90	0.93	0.90	0.88

27	29	32	33	34	35	36	37	38	41	42	43	44	46	47	48	49	51	53	54	55
0.20	0.26	0.20	0.20	0.21	-0.19	0.25	0.21	0.21	0.20	-0.20	0.20	0.21	0.19	-0.19	0.20	-0.20	0.21	-0.21	0.18	0.21
-0.22	0.26	-0.22	-0.22	-0.23	-0.21	0.25	-0.22	-0.21	-0.22	-0.20	-0.22	-0.23	-0.20	-0.22	-0.22	-0.20	-0.23	-0.23	0.20	-0.22
-0.24	0.28	-0.23	0.24	0.25	-0.23	0.26	0.24	0.22	-0.22	-0.24	-0.23	0.26	-0.22	0.24	0.24	-0.24	0.25	-0.25	-0.21	0.23
-0.23	-0.24	0.22	-0.22	-0.21	-0.21	0.28	-0.21	0.23	0.22	-0.21	0.21	-0.24	0.21	-0.21	-0.22	-0.20	-0.22	-0.24	0.21	0.23
-0.25	-0.26	-0.23	0.24	-0.23	-0.24	-0.26	0.24	-0.25	0.23	-0.23	-0.22	-0.28	-0.23	-0.24	-0.24	-0.25	-0.24	-0.25	-0.23	-0.25
-0.19	0.22	0.20	0.22	-0.19	-0.19	0.22	0.22	0.19	0.21	-0.19	0.17	0.24	-0.18	-0.18	0.19	-0.19	-0.19	0.20	-0.17	0.22
-0.22	-0.22	0.20	-0.22	-0.20	-0.20	0.29	-0.20	0.21	-0.20	-0.19	-0.19	-0.23	0.18	-0.20	-0.21	-0.19	-0.21	-0.23	-0.20	0.22
-0.22	0.21	0.20	-0.21	0.22	-0.19	0.27	-0.20	0.21	0.20	0.18	0.19	-0.23	0.19	-0.20	-0.20	0.20	-0.21	-0.22	0.22	0.21
-0.25	0.22	-0.23	-0.25	-0.21	-0.21	0.29	-0.25	-0.24	-0.23	-0.21	0.21	-0.28	-0.20	-0.25	-0.25	-0.23	-0.24	-0.25	-0.24	-0.25
0.23	0.23	0.21	0.23	0.22	-0.20	0.23	0.22	0.21	0.21	-0.19	0.19	-0.25	-0.19	0.22	0.22	-0.22	0.23	-0.22	0.21	0.22
-0.21	0.24	0.20	-0.20	0.21	-0.20	-0.23	0.21	0.20	0.20	0.18	0.20	0.22	-0.19	-0.21	-0.21	-0.22	0.21	-0.21	-0.19	0.21
-0.23	0.22	-0.21	-0.23	0.21	-0.20	0.28	-0.23	0.21	0.21	-0.19	0.19	-0.26	0.19	-0.22	-0.23	-0.21	0.22	-0.23	-0.22	-0.23
-0.23	0.24	0.25	0.24	-0.29	-0.26	0.29	0.23	0.23	-0.24	-0.28	0.23	-0.25	-0.27	-0.25	-0.23	-0.26	-0.27	-0.24	-0.23	-0.24
-0.27	0.27	-0.26	0.26	-0.30	-0.29	0.31	0.26	0.24	-0.26	-0.30	-0.25	0.27	-0.29	-0.27	-0.26	-0.28	-0.28	-0.26	-0.25	0.26
0.97	0.82	0.94	0.94	0.91	0.96	0.83	0.91	0.91	0.92	0.94	0.92	0.88	0.91	0.92	0.95	0.94	0.94	0.91	0.88	0.90
0.96	0.84	0.95	0.93	0.96	0.98	0.84	0.92	0.95	0.96	0.97	0.96	0.89	0.95	0.95	0.97	0.97	0.97	0.93	0.91	0.91
0.92	0.84	0.95	0.92	0.96	0.96	0.81	0.90	0.94	0.95	0.96	0.96	0.87	0.96	0.95	0.95	0.95	0.97	0.93	0.94	0.91
0.93	0.86	0.93	0.91	0.98	0.95	0.81	0.89	0.91	0.93	0.94	0.94	0.87	0.95	0.97	0.95	0.97	0.99	0.93	0.94	0.90
0.98	0.81	0.97	0.96	0.92	0.96	0.85	0.93	0.95	0.96	0.93	0.94	0.93	0.92	0.95	0.97	0.97	0.96	0.94	0.89	0.93
0.98	0.84	0.92	0.93	0.92	0.93	0.80	0.89	0.92	0.92	0.92	0.92	0.93	0.90	0.96	0.97	0.96	0.97	0.91	0.89	0.90
0.91	0.85	0.92	0.89	0.97	0.95	0.79	0.86	0.90	0.91	0.96	0.94	0.84	0.96	0.95	0.93	0.94	0.96	0.91	0.94	0.88
1.00	0.80	0.96	0.97	0.89	0.94	0.85	0.94	0.93	0.94	0.91	0.92	0.94	0.88	0.94	0.98	0.96	0.95	0.94	0.88	0.94
0.80	1.00	0.78	0.75	0.88	0.82	0.64	0.72	0.78	0.79	0.85	0.81	0.75	0.84	0.83	0.82	0.84	0.86	0.77	0.80	0.74
0.96	0.78	1.00	0.97	0.90	0.96	0.85	0.96	0.98	0.98	0.92	0.96	0.93	0.92	0.93	0.95	0.95	0.94	0.97	0.92	0.97
0.97	0.75	0.97	1.00	0.87	0.93	0.86	0.98	0.93	0.96	0.87	0.90	0.96	0.87	0.92	0.95	0.95	0.92	0.95	0.87	0.96
0.89	0.88	0.90	0.87	1.00	0.93	0.77	0.85	0.89	0.90	0.96	0.93	0.83	0.96	0.95	0.93	0.95	0.97	0.90	0.93	0.86
0.94	0.82	0.96	0.93	0.93	1.00	0.82	0.91	0.95	0.96	0.97	0.97	0.87	0.95	0.94	0.96	0.95	0.95	0.94	0.92	0.93
0.85	0.64	0.85	0.86	0.77	0.82	1.00	0.86	0.81	0.84	0.78	0.80	0.80	0.78	0.81	0.84	0.83	0.81	0.84	0.78	0.84
0.94	0.72	0.96	0.98	0.85	0.91	0.86	1.00	0.93	0.96	0.86	0.89	0.95	0.86	0.91	0.93	0.93	0.90	0.96	0.87	0.97
0.93	0.78	0.98	0.93	0.89	0.95	0.81	0.93	1.00	0.98	0.93	0.96	0.90	0.92	0.93	0.95	0.94	0.93	0.95	0.91	0.95
0.94	0.79	0.98	0.96	0.90	0.96	0.84	0.96	0.98	1.00	0.94	0.96	0.93	0.93	0.94	0.96	0.96	0.94	0.98	0.92	0.98
0.91	0.85	0.92	0.87	0.96	0.97	0.78	0.86	0.93	0.94	1.00	0.97	0.83	0.99	0.94	0.94	0.95	0.95	0.92	0.92	0.88
0.92	0.81	0.96	0.90	0.93	0.97	0.80	0.89	0.96	0.96	0.97	1.00	0.87	0.97	0.95	0.95	0.95	0.94	0.95	0.94	0.93
0.94	0.75	0.93	0.96	0.83	0.87	0.80	0.95	0.90	0.93	0.83	0.87	1.00	0.82	0.91	0.94	0.93	0.91	0.94	0.84	0.95
0.88	0.84	0.92	0.87	0.96	0.95	0.78	0.86	0.92	0.93	0.99	0.97	0.82	1.00	0.95	0.93	0.95	0.95	0.92	0.95	0.89
0.94	0.83	0.93	0.92	0.95	0.94	0.81	0.91	0.93	0.94	0.94	0.95	0.91	0.95	1.00	0.97	0.98	0.98	0.95	0.96	0.93
0.98	0.82	0.95	0.95	0.93	0.96	0.84	0.93	0.95	0.96	0.94	0.95	0.94	0.93	0.97	1.00	0.99	0.98	0.96	0.93	0.95
0.96	0.84	0.95	0.95	0.95	0.95	0.83	0.93	0.94	0.96	0.95	0.95	0.93	0.95	0.98	0.99	1.00	0.98	0.96	0.93	0.93
0.95	0.86	0.94	0.92	0.97	0.95	0.81	0.90	0.93	0.94	0.95	0.94	0.91	0.95	0.98	0.98	0.98	1.00	0.94	0.93	0.91
0.94	0.77	0.97	0.95	0.90	0.94	0.84	0.96	0.95	0.98	0.92	0.95	0.94	0.92	0.95	0.96	0.96	0.94	1.00	0.94	0.99
0.88	0.80	0.92	0.87	0.93	0.92	0.78	0.87	0.91	0.92	0.92	0.94	0.84	0.95	0.96	0.93	0.93	0.93	0.94	1.00	0.91
0.94	0.74	0.97	0.96	0.86	0.93	0.84	0.97	0.95	0.98	0.88	0.93	0.95	0.89	0.93	0.95	0.93	0.91	0.99	0.91	1.00

REFERENCES

AZZARO, R. and M.S. BARBANO (2000): Analysis of the seismicity of Southeastern Sicily: a proposed tectonic interpretation, *Ann. Geofis.*, **43** (1), 171-188.

AMATO, A., R. AZZARA, A. BASILI, C. CHIARABBA, M. COCCO, M. DI BONA and G. SELVAGGI (1995): Main shock and aftershocks of the December 13, 1990, Eastern Sicily earthquake, *Ann. Geofis.*, **38** (2), 255-266.

BEN AVRAHAM, Z., V. LYAKHOVSKY and M. GRASSO (1995): Simulation of collision zone segmentation in the Central Mediterranean, *Tectonophysics*, **243**, 57-68.

BIANCA, M., C. MONACO, L. TORTORICI and L. CERNOBORI (1999): Quaternary normal faulting in Southeastern Sicily (Italy): a seismic source for the 1693 large earthquake, *Geophys. J. Int.*, **139**, 370-394.

BOSCHI, E., E. GUIDOBONI and D. MARIOTTI (1995): Seismic effects of the strongest historical earthquakes in the Syracuse area, *Ann. Geofis.*, **38** (2), 223-253.

BOSCHI, E., E. GUIDOBONI, G. FERRARI, G. VALENSISE and P. GASPERINI (Editors) (1997): *Catalogo dei Forti Terremoti in Italia dal 461 a.C. al 1990* (ING, Roma - SGA, Bologna), pp. 644.

CARBONE, S., M. GRASSO and F. LENTINI (1987): Lineamenti geologici del plateau Ibleo (Sicilia SE). Presentazione delle carte geologiche della Sicilia Sud-Orientale, *Mem. Soc. Geol. It.*, **38**, 127-135.

COGAN, J., L. RIGO, M. GRASSO and I. LERCHE (1989): Flexural tectonics of Southeastern Sicily, *J. Geodyn.*, **11**, 189-241.

GRASSO, M. and C.D. REUTHER (1988): The western margin of Hyblean plateau: a neotectonic trasform system on the SE Sicilian foreland, *Ann. Tectonicae*, **II** (2), 107-120.

HIRN, A., R. NICOLICH, J. GALLART, M. LAIGLE, L. CERNOBORI and ETNASEIS SCIENTIFIC GROUP (1997): Roots of Etna volcano in faults of great earthquakes, *Earth Planet. Sci. Lett.*, **148**, 171-191.

LAHR, J.C. (1989): HYPOELLIPSE/VERSION 2.0: A computer program for determining local earthquake hypocentral parameters, magnitude, and first motion pattern, *U.S. Geol. Surv., Open-File Rep. 89/116*, pp. 81.

LENTINI, F., S. CARBONE and S. CATALANO (1994): Main structural domains of the Central Mediterranean region and their tectonic evolution, *Boll. Geofis. Teor. Appl.*, **36** (141-144), 103-125.

LENTINI, F., S. CARBONE, S. CATALANO and M. GRASSO (1996): Elementi per la ricostruzione del quadro strutturale della Sicilia Orientale, *Mem. Soc. Geol. It.*, **38**,127-135.

MÜLLER, B., M.L. ZOBACK, K. FUCHS, L. MASTIN, S. GREGERSEN, N. PAVONI, O. STEPHANSSON and C. LJUNGGREN (1992): Regional patterns of tectonic stress in Europe, *J. Geophys. Res.*, **97**, 11783-11803.

RAGG, S., M. GRASSO and B. MÜLLER (1999): Patterns of tectonic stress in Sicily from borehole breakout observations and finite element modeling, *Tectonics*, **18** (4), 669-685.

REASENBERG, P.A. and D. OPPENHEIMER (1985): FPFIT, FPPLOT and FPPAGE: Fortran computer programs for calculating and displaying earthquakes fault-plane solutions, *U.S. Geol. Surv., Open-File Rep. 85/739*, pp. 109.

RICHARDSON, R.M., S.C. SOLOMON and N.H. SLEEP (1979): Tectonic stress in the plates, *Rev. Geophys.*, **17**, 981-1019.

RICHTER, C.F. (1958): *Elementary Seismology* (Freeman, San Francisco), pp. 768.

SCANDONE, P., E. PATACCA, R. RADOICIC, W.B.F. RYAN, M.B. CITA, M. RAWSON, H. CHEZAR, E. MILLER, J. MCKENZIE and S. ROSSI (1981): Mesozoic and Cenozoic rocks from Malta escarpment (Central Mediterranean), *Am. Ass. Petr. Geol. Bull.*, **65**, 1299-1319.

SCHERBAUM, F. and J. JOHNSON (1992): Programmable interactive toolbox for seismological analysis, *IASPEI Software Library*, edited by W.H.K. LEE.

SHARP, A.D.L., P.M. DAVIS, F. GRAY and G.C.P. KING (1980): Preliminary results from a seismic array study of Mount Etna, *United Kingdom Research on Mount Etna, 1977-1979*, The Royal Society, London, 15-18.

SIROVICH, L. and F. PETTENATI (1999): Seismotectonic outline of South-Eastern Sicily: an evaluation of available options for the earthquake fault rupture scenario, *J. Seismol.*, **3** (3), 213-233.

WARD, S.N. (1994): Constraints on the seismotectonics of the Central Mediterranean from very long baseline, *Geophys. J. Int.*, **117**, 441-452.

YELLIN-DROR, A., M. GRASSO, Z. BEN-AVRAHAM and G. TIBOR (1997): The subsidence history of the Northern Hyblean Plateau margin, Eastern Sicily, *Tectonophysics*, **282**, 277-289.

(received January 11, 2001;
accepted June 15, 2001)